What is the most important mechanical factor involved in trapeziometacarpal osteoarthritis development? A sensitivity analysis based on biomechanical modelling

Thomas Valerio, Jean-Louis Milan, Benjamin Goislard de Monsabert, Laurent Vigouroux

What is the most important mechanical factor involved in trapeziometacarpal osteoarthritis development? A sensitivity analysis based on biomechanical modelling

Thomas Valerio[a,b], Jean-Louis Milan[a,b], Benjamin Goislard de Monsabert[a] and Laurent Vigouroux[a]

[a] CNRS, ISM, Aix-Marseille University, Marseille, France; [b] APHM, CNRS, ISM, St Marguerite Hospital, Institute for Locomotion, Department of Orthopaedics and Traumatology, Aix-Marseille University, Marseille, France

ABSTRACT

Few studies consider the variability of the model parameters. This study aimed to perform a sensitivity analysis of a trapeziometacarpal joint model, by performing 675 finite element simulations built from the combination of different morphologies, joint passive stiffness, and grip strategies to estimate the joint pressure. Pressure variability was significantly more affected by morphology than grip strategy and joint passive stiffness. The effect of morphology and grip strategy on joint pressure was significant. A significant correlation between the trapezium dorso-volar curvature and the joint pressure was found. Morphology seems more important than the other parameters to estimate joint contact pressure correctly.

KEYWORDS

Trapeziometacarpal osteoarthritis; bone morphology; muscles forces; joint passive stiffness; contact pressures

Introduction

The trapeziometacarpal (TMC) joint, is one of the most joint affected by osteoarthritis (OA) in the body (Cvijetic et al. 2004). The joint mechanical loading, i.e. contact force and pressure applied on the joint cartilages, appears as one important factor potentially explaining the apparition and progression of this pathology (Felson 2013; Droz-Bartholet et al. 2016). The mechanical pathway that contributes to TMC OA appearance is studied using biomechanical models that are developed based on finite element (FE) models using imaging data to obtain bone and cartilage geometry. Boundary conditions to simulate the grasping task are applied to the FE models (Schneider et al. 2017; Dong et al. 2023; Valerio et al. 2023) by integrating muscle forces or joint reaction forces previously estimated by multi-body rigid models
(Goislard de Monsabert et al. 2014; Barry et al. 2018). The joint contact pressure can then be estimated through this modelling approach to determine OA risk factors in various configurations of grip tasks or various anatomical characteristics. Previous studies have shown that different bone morphology, joint passive stiffness, hand surgical intervention, or hand therapy may influence the joint contact pressure on the TMC joint (Dong et al. 2023; Valerio et al. 2023, 2024). These previous studies corroborate previous clinical investigations about the potential importance of these parameters in OA development (Jonsson et al. 2009; Ladd et al. 2014; Sim et al. 2022). Nevertheless, while testing the effect of these parameters separately, the effect of the interaction between the parameters and the hierarchy between the importance of each parameter is still unknown. To investigate this interaction, a thorough methodology is needed to determine a range of realistic variability of parameters and their propagation on the variability to the outputs, i.e. joint contact forces and pressures. The most commonly used methods are factorial analysis, Taguchi method, or Monte Carlo analysis (Mangado et al. 2016). For example, a previous study by Yang et al. (2007) found that the morphology of the cervical ring cage explained more von Mises stress variation than its material properties *via* the Taguchi method. As another example, (Espino et al. 2003) established similar conclusions for the intervertebral disc through a factorial analysis with a higher effect of morphology than material properties or vertebral compressive force scenario.

Based on the same kind of approach, the present study aimed to understand the contribution of several crucial identified factors on the contact pressure of the TMC joint and their interaction to look at the overall potential risk of these factors on the OA development. A sensitivity analysis was performed on three main factors with an important effect on joint contact pressure and a potential mechanical effect on TMC OA development, according to previous literature. We hypothesized that all the parameters had a significant effect on joint contact pressure variability and a significant interaction effect between them. Especially, we hypothesized that morphology was the most important parameter among the others to explain mean joint contact pressure variability as it was observed in other musculoskeletal systems (Espino et al. 2003; Yang et al. 2007).

Materials and methods

Finite element model of the thumb setup

A template thumb model was developed at first, and the main parameters of this model (morphology, joint position, spring stiffness) were changed to perform the sensitivity analysis (see next part). The template thumb model was developed based on a CT-scan of one participant (slice thickness: 0.625 mm; pixel size: 0.372 mm; resolution:512 px 512 px) realized in the pinch grip task. This CT-scan came from a previous study of our group (Faudot et al. 2020). The thumb bone geometries were obtained by segmentation using Mimics (Research 22.0; Materialise, Belgium). This model includes the trapezium, the metacarpal bone, and the two phalanges (Figure 1a). The bones were meshed using non-linear tetrahedral elements of 10 nodes with an edge length of 1.3 mm. Cartilage was then created by extruding the subchondral bone surface manually identified to create prismatic elements (three layers were used). The thickness of the cartilage for the TMC joint was considered constant with a size of 0.7 mm (Koff et al. 2003; Dourthe et al. 2019). Each prismatic element consisted of quadratic pentagonal elements of 15 nodes with an average triangle size of 1.3 mm and thickness of 0.23 mm. The number of elements for the cartilage ranged from 345 to 909 elements according to the morphology modeled. Cartilage Mesh quality metrics were verified with a Jacobian higher than 0.4 for 98% of elements, an aspect ratio under 3 for 96% of elements, and an angle asymmetry higher than 0.5 for 95% of elements. Three elements deep were used to model the cartilage thickness, defined after mesh convergence. The bone was considered as rigid body and the cartilage was modeled by a neo-Hookean hyperelastic material property (E ¼ 10 MPa, v ¼ 0.4) (Kempson 1972; Schneider et al. 2017; Dong et al. 2023). A neo-

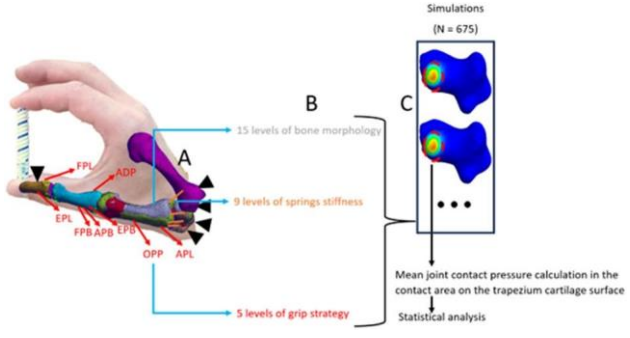

Figure 1. The sensitivity analysis performed on the thumb FE model. This figure shows the thumb finite element model used in this study (a), the factors and their levels for the sensitivity analysis (b), and the analysis of the model outputs (c). The black triangles represent the boundary conditions of the FE model, which were the removal of degrees of freedom in all directions for the trapezium and second metacarpal bone and the removal only in the direction of the force applied for the distal phalanx. The muscle forces applied as boundary conditions are represented by red arrows to simulate each grip strategy (Table 1). For the grip strategy factor, it should be noted that not only the muscle forces were changed but also the bone joint positions to simulate different joint angles during a pinch grip task.

Hookean model is defined by the following strain energy density function:

$$W = C_{10}(I_1 - 3)\left(J - 1\right)^2 + \frac{1}{D_1}$$

In this equation, C_{10} is a material constant related to the shear modulus, D_1 is the first invariant of the right Cauchy-Green deformation tensor, and J is the determinant of the deformation gradient. The coefficients C_{10} and D_1 could be calculated from E and v, by using the following equations:

$$C_{10} = \frac{E}{4(1+\nu)}$$

$$D_1 = \frac{6(1-2\nu)}{E}$$

A sliding elastic contact implemented with a penalty-type method was used to ensure cartilage contact during the simulation (Maas et al. 2012; Zimmerman and Ateshian 2018; Dong et al. 2023). The TMC joint passive stiffness was modeled by nine linear springs placed all around the joint to represent the global stiffness caused by the ligament, the joint capsule, the subcutaneous tissues, and the skin. Other linear springs with a value of 100,000N/mm were used for the two distal joints to ensure model stability. Thumb muscle attachment surfaces were manually identified on the bones and a force vector was applied on the surface with a direction determined by the muscle moment arms. This technique was

Table 1. The muscle forces values and the TMC joint position for the five pinch grip strategies simulated in the grip strategy factor for the sensitivity analysis (G1, G2, G3, G4, and G5). The thumb muscles presented here are the flexor pollicis longus (FPL), the flexor pollicis brevis (FPB), the opponens pollicis (OPP), the abductor pollicis brevis (APB), the adductor pollicis (ADP), the abductor pollicis longus (APL), the extensor pollicis longus (EPL) and the extensor pollicis brevis (EPB). The TMC joint angles correspond to the flexion-extension angle (F), the adduction-abduction angle (A) and the pronation-supination angle (P). A positive angle indicates a position in flexion, abduction, and pronation respectively. The five grip strategies

represent the five levels of the grip strategy factor. These data came from (Goislard de Monsabert et al. 2014).

		Grip strategies				
		G1	G2	G3	G4	G5
Muscle forces (N)	FPL	133,2	188.4	106.8	191.0	139.4
	FPB	0.0	0.0	0.0	0.0	0.0
	OPP	472.7	338.6	289.0	388.6	512.1
	APB	163.3	187.1	58.7	184.4	255.9
	ADP	159.8	74.6	151.9	95.4	93.1
	APL	107.2	166.0	0.0	96.1	282.2
	EPL	99.9	149.9	150.0	107.7	0.0
	EPB	0.0	0.0	0.0	0.0	0.0
TMC joint angles ()	F	6.6	5.9	14.4	11.8	−1.4
	A	−14.5	−15.1	−15.9	−6.7	−5.6
	P	7.4	4.1	9.5	14.0	6.2

inspired by Dong et al. (2023). The values of each muscle forces were determined from a multi-body rigid model developed in our group (Goislard de Monsabert et al. 2014). This model used joint angles and pinch grip force as input to determine the corresponding muscle forces by solving mechanical equations and using an optimization procedure based on a muscle stress criterion (Goislard de Monsabert et al. 2014). The thumb muscles considered in this model are shown in Table 1. The trapezium bone was fixed in all degrees of freedom, considering its weak movement in comparison with the metacarpal bone (Sciacca et al. 2022). The movement in the direction perpendicular to the thumb tip force applied was also removed. FE simulations were run using FEBio (Maas et al. 2012) with the default convergence criteria. Displacement, energy, residual, and line search tolerances were set at 0.001, 0.01, 0, and 0.9 respectively, the minimal residual error was set at 1^{-20} and the Broyden-Fletcher-Goldfarb- Shanno quasi-Newton method was used. The bone morphology, muscle forces/joint position, and spring stiffness were modified in this template model to perform the sensitivity analysis (see next part).

Choice of factor and level for the sensitivity analysis

The summary of the methodology developed to achieve the sensitivity analysis is described in Figure 1. To represent all the configuration possibilities in the population, 15 levels were simulated for the morphology factor, 5 levels were selected for the grip strategy factor and 9 levels were selected for the joint passive stiffness factor, which represent a total of 675 simulations for the sensitivity analysis. The 15 different TMC joint bone morphologies were taken from the segmentation of 15 CT-scans originating from a previous study of our group (Valerio et al. 2023). The segmentation operator and the CT-scan resolution were the same as the template model. The bones models were registered in the same pinch grip position as the template model with the iterative closest point algorithm (Besl and McKay 1992; Cerveri et al. 2010; Valerio et al. 2023). These bone morphologies were chosen because the morphological parameters (size and curvature) are consistent with more population sample and representative of the population (Halilaj et al. 2014; Shih et al. 2018; Rusli and Kedgley 2020; Athlani et al. 2021; Valerio et al. 2023). After the bone's registration, bones were meshed, and cartilage was created using the same techniques as the template model. The two distal phalanxes of the template model were unchanged in order to focus on the effect of TMC joint morphology only. The muscle attachment surfaces manually identified on the metacarpal bone of the template model were used to select the triangles of the mesh of the 15 other bones closest to the triangle of the template mesh. New linear springs were created for the 15 registered bones, based on the linear springs of the template model with the same direction and position around the joint. 9 stiffness combinations were used for the nine linear springs in order to investigate the sensitivity of the joint passive stiffness. These different combinations of stiffness values were determined by laxity tests performed on different participants and an optimization method to fit the force-displacement data of the laxity tests with the FE model. A more detailed description of this joint passive stiffness modelling method is described in a previous study of our group (Valerio et al. 2024). The stiffness values of the FE model springs are presented in Table 2. 5 different grip strategies were simulated in the finite element model. The 5 grip strategies were selected from a previous experiment in which kinematic and grip force were recorded and the thumb muscle forces were estimated by the multi-body rigid model (Goislard de

Monsabert et al. 2014). The 5 grip strategies correspond to 5 different participants chosen among ten participants to reduce the number of simulations given that some participants had similar joint angles and muscle forces. A K-mean clustering was performed on the data to isolate the different groups of pinch grip strategies. The different muscle forces of the 5 grip strategies are presented in Table 1. The muscle forces were applied on the thumb model as boundary conditions to simulate the different grip strategies and the position of the bones in the model was also modified in order to fit the positions recorded by the kinematic analysis of Goislard de Monsabert et al. (2014). The muscles forces were applied on the insertion surfaces manually identified on each model with a vector representing the muscle action, considering its moment arm and anatomy (Van Arkel et al. 2013). During each of the 675 simulations, the contact pressure (the average of the principal stresses) was averaged on the trapezium cartilage surface in the joint contact area (Figure 1c).

Table 2. The stiffness value of each linear spring for the different linear spring's combinations used in the sensitivity analysis. The stiffness values are presented in N.mm^{-1}. This table presents the value and the location of the nine linear springs to model the TMC joint passive stiffness for nine different participants with different TMC joint laxity. The nine different participants represent the nine levels of factor for the joint passive stiffness.

		Participant								
	Spring location	P1	P2	P3	P4	P5	P6	P7	P8	P9
Spring 1	Dorso-Central	5.1	16.8	24.7	24.7	5.4	12.8	18.8	24.5	5.0
Spring 2	Dorso-Ulnar	23.7	5.5	11.9	23.1	9.5	24.7	24.5	24.2	24.5
Spring 3	Ulno-Volar	5.1	24.4	24.6	5.4	21.0	21.8	10.6	5.0	24.8
Spring 4	Centro-Volar	15.2	11.0	8.3	19.5	12.3	4.9	24.4	18.7	24.9
Spring 5	Centro-Radial	5.1	20.0	4.9	22.2	7.0	4.9	6.8	13.0	6.2
Spring 6	Dorso-Radial	20.3	5.0	5.0	19.8	14.2	4.9	24.5	12.3	16.1
Spring 7	Centro-Volar	17.0	11.6	24.5	11.6	4.9	7.0	23.5	4.9	20.9
Spring 8	Dorso-Radial	5.0	5.6	5.2	16.6	23.3	4.9	24.7	4.9	25.0
Spring 9	Radio-Volar	9.1	21.8	24.7	6.1	24.3	24.7	24.6	24.7	25.0
Sum		105.7	121.6	133.9	149.0	122.0	110.9	182.6	132.4	172.4

Statistical analysis

Joint contact pressure results were analysed through an analysis of variance (ANOVA) to investigate the effect of the three parameters studied: the morphology, the grip strategy, and the joint passive stiffness, and the interaction between those parameters. The regression coefficients were also determined for each parameter to determine the change in the main response of the joint pressure due to a parameter when the other parameters were constant. This regression coefficient was calculated by dividing the variance explained by the parameter by the global variance in the dataset. A linear regression analysis was also performed between the trapezium dorso- volar curvature of each morphology and the average of the joint pressure for each morphology to see if the important effect of morphology reported in Valerio et al. (2023) was confirmed with more simulations. A Pearson test was used to determine the significance of the correlation between the curvature and the pressure. The significance threshold was set at $p < 0.05$ for the ANOVA and the correlation test.

The Python modules Scipy 1.10.1 and Statsmodels 0.13.2 were used for the statistical analysis.

Results

Joint contact pressure for each level of factor

From the 675 simulations performed, 491 terminated successfully. The complete table resuming all the simulations and the scenarios that did not converge is available in Supplementary Materials (Table 4–Supplementary Materials). The 184 aborted simulations are due to excessive loading on the cartilage edge which caused convergence problems on the elements. Only the data from these 491 converging simulations thus are presented in the following results. The value of the mean contact pressure of the TMC joint averaged 7.8 ± 1.3 MPa (range: 4.5 − 10.9 MPa) for all the simulations. Mean TMC pressure values ranged from 5.0 to 10.0 MPa for the 15 morphologies, from 6.9 to 8.5 MPa for the 5 grip strategies, and from 7.6 to 7.9 MPa for the 9 joint passive stiffness. A 4D plot of the results from the 491 converging simulations is shown in Figure 2.

Analysis of variance

The results from the ANOVA are presented in Table 3. Morphology and grip strategies had a significant effect on the contact pressure of the TMC joint (Morphology: F ¼ 1578.4, p ¼ 1.1^{-16}; Grip strategies: F ¼ 102.0, p ¼

1.1^{-16}) but not joint passive stiffness (F ¼ 3.9, p ¼ 0.05). A significant interaction was found between the morphology and the grip strategies (F ¼ 6633.7, p ¼ 1.1^{-16}), between the morphology and the joint passive stiffness (F ¼ 910.9, p ¼ 1.1^{-16}), and

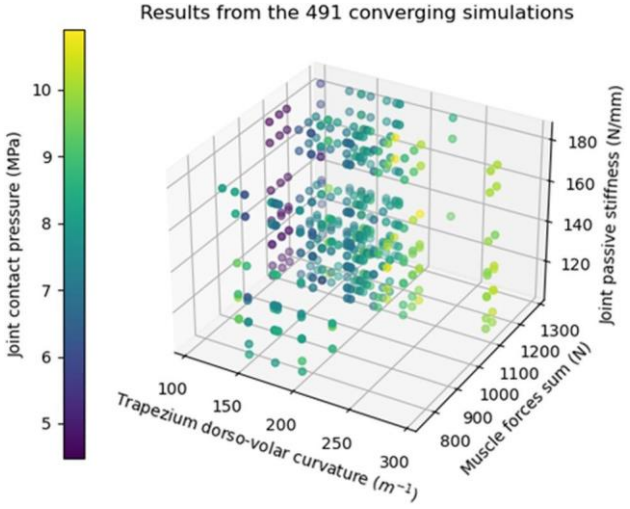

Figure 2. 4D scatter plot of the 491 results from the simulations that terminated successfully. The morphology is summarized by the trapezium dorso-volar curvature, the grip strategy is summarized by the sum of the thumb muscle forces, and the joint passive stiffness is summarized by the sum of the spring's stiffness. The points represented correspond to the average contact stress for each parameter combination.

Table 3. The p value of each factor and the interaction. These results came from the ANOVA performed on the 491 complete simulations with a 95% confidence interval.

Factor	*P* value
Morphology	1.1-16
Grip strategy	1.1-16
Joint passive stiffness	0.05
Morphology: Grip strategy	1.1-16
Morphology: Joint passive stiffness	1.1-16
Grip strategy: Joint passive stiffness	1.0-4

between the grip strategies and the joint passive stiffness (F ¼ 59.1, p ¼ 1.0^{-4}). Morphology had a most important effect on joint contact pressure variability (r^2 ¼ 0.70) than grip strategies (r^2 ¼ 0.13) and joint passive stiffness (r^2 ¼ 0.01) (Figure 3).

Relationship between morphology curvature and joint contact pressure

The plot of the linear regression model performed between the trapezium dorso-volar curvature and the mean values of the contact pressure of the TMC joint for each morphology is presented in Figure 4. The relationship between the contact area and the joint pressure is presented in Figure 5. Pearson test reveals a significant effect of the trapezium dorso-volar curvature on the contact pressure of the TMC joint (r^2 ¼ 0.64; p ¼ 0.0003). An important correlation was also found between the contact area and the joint pressure (r^2 ¼ 0.85; p ¼ 0.000001).

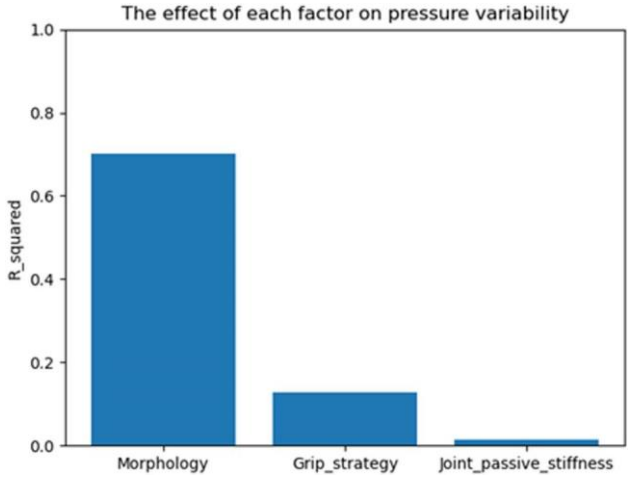

Figure 3. R_squared value of each factor from the ANOVA. This R_squared is calculated from the ANOVA F value. A value of 1 indicates an important contribution of the parameter on the pressure variability and a value of 0 indicates a poor contribution.

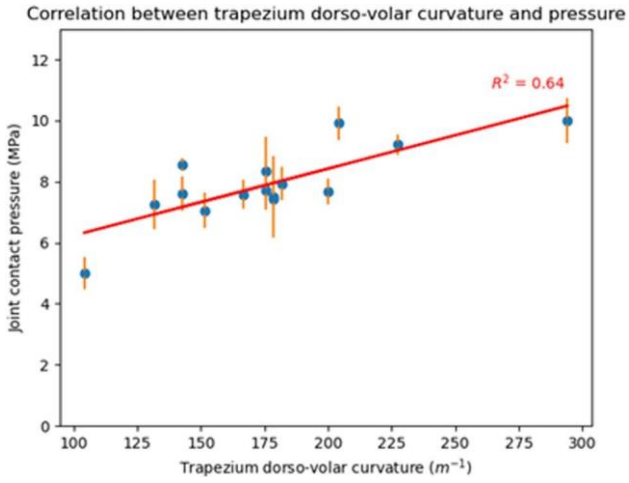

Figure 4. The linear regression between the trapezium dorso-volar curvature and the average of the contact pressure of the TMC joint for each morphology. The blue points represent the joint contact pressure for each morphology, averaged for the different levels of grip strategy and joint passive stiffness. The orange bar represents the standard deviation. The regression line is represented by the red line. The trapezium dorso- volar curvatures were measured for each morphology with the methodology of Valerio et al. (2023).

Discussion

The objectives of this study were to evaluate the combined effect of the TMC joint bone morphology, the grip strategy, and the joint passive stiffness on the pressure endured by the cartilage to understand OA

development. A sensitivity analysis was performed on a thumb FE model by modifying each parameter through a factorial analysis to investigate all the combinations of parameters. Each factor was investigated

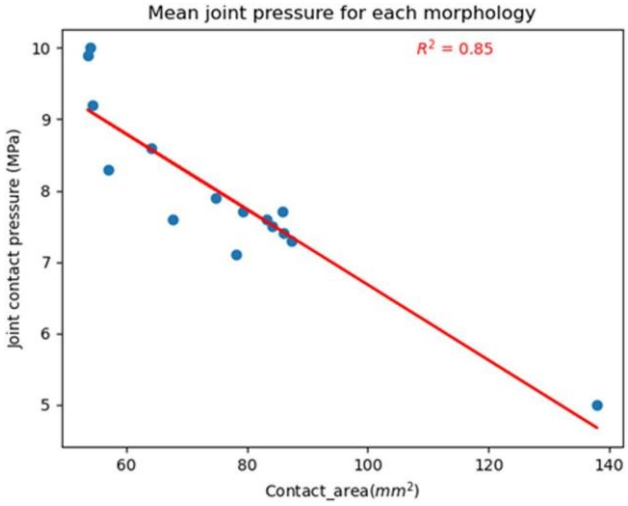

Figure 5. The linear regression between the contact area and the average of the contact pressure of the TMC joint for each morphology. The blue points represent the joint contact pressure for each morphology, averaged for the different levels of grip strategy and joint passive stiffness. The regression line is represented by the red line.

from values determined from different *in vivo* medical imaging and motion dataset captures providing a physiological range of each parameter.

491 simulations terminated successfully satisfying default convergence criteria. Another previous study on the FE modelling of TMC joint had the same kind of problem for some conditions tested (van Leeuwen et al. 2021). This denoted that the model is not able to simulate all the configurations, especially the ones involving high lateral displacement of the TMC joint. It is not possible to draw any conclusions from these 184 aborted simulations, nor to say that they correspond to extreme values for any of the 3 factors, or that they correspond to incompatible sets of parameters. A possible explanation is thus that a specific combination of factors results in non-physiological situations, for instance, that applying a specific muscle force coordination and posture is not physiological for some morphologies resulting in aberrant simulation that cannot converge. No common pattern of factors could be identified to explain the scenarios that did not converge. It will be interesting to further investigate these aborted configurations in future studies and find the threshold where this simulation could run and thus would become physiological. The conclusions of the study thus are based on the only simulations that have converged.

The contact pressure of the TMC joint values estimated from the 491 converging simulations agreed fairly well and consistent with previous literature with the same kind of modelling approach and simulated pinch grip task (Goislard de Monsabert et al. 2014; Valerio et al. 2023). The mean joint contact pressure of the TMC joint for all the simulations in this study decreased by 5% from (Goislard de Monsabert et al. 2014) and decreased by 50% from (Valerio et al. 2023). Considering that the pinch grip task used as input for all these studies was the same, the important differences from (Valerio et al. 2023) can be explained by the difference in modelling approaches. (Goislard de Monsabert et al. 2014) estimated the TMC joint pressure by calculating the TMC joint reaction force from an multi-body rigid model and then by dividing the force by the TMC joint contact area identified on MRI. On the other side, (Valerio et al. 2023) used a simplified TMC joint model with only the trapezium and first metacarpal bone modeled and the TMC joint reaction force was applied as boundary conditions. The metacarpal bone was constrained to move only in the direction of the TMC joint force in Valerio et al. (2023) while the metacarpal bone in this study was unconstrained and controlled by the muscle forces and the springs element. Restraining the movement in the direction of the TMC joint reaction force in Valerio et al. (2023) can thus lead to a non-physiological contact and thus increase the pressure on cartilage. Despite the differences in pressure values, the data from the converging simulations showed a correlation between the trapezium dorso-volar curvature and the contact pressure of the TMC joint (Figure 4), as already observed (Valerio et al. 2023). In this former study, (Valerio et al. 2023) found a significant correlation between the trapezium dorso-volar curvature and the TMC joint pressure during the pinch grip task with an r^2 value of 0.62, against 0.64 in this study. The relationship observed in this study with a larger number of simulations confirms the TMC bone morphology effects on the joint contact pressure and highlights the large potential of this factor to contribute to OA development. This effect of trapezium dorso-volar curvature on pressure could also explain the prevalence of TMC OA in women (Moriatis Wolf et al. 2014) since previous studies reported higher curvature for women (Ateshian et al. 1992; Xu et al. 1998; Halilaj et al. 2014). A previous used a similar approach to estimate the joint pressure on the TMC joint through FE modelling (Kurosawa et al. 2024). This study analysed the effect of the TMC joint dorso-volar and ulno-radial congruence on joint pressure. They defined these congruences as the

ratio between the corresponding curvature of the two subchondral bone surfaces (first metacarpal and trapezium). Interestingly, they found a significant correlation between dorso-volar congruence and joint pressure. The dorso-volar direction could thus be an interesting direction to investigate and further studies need to clarify why there is more effect of TMC morphology in the dorso-volar direction.

Results from the ANOVA showed a significant effect of morphology and grip strategy on the contact pressure of the TMC joint but not a significant effect of joint passive stiffness (Table 3). The significant effect of grip strategy on the TMC joint pressure is interesting from a clinical point of view because these findings support the idea that patient-specific grip strategies could potentially lead to joint overloading and thus be part of the risk of OA degenerative progression. For instance, from a rehabilitation or prevention perspective, it would be interesting to identify whether TMC joint pressure could be decreased by recommending specific grip strategies leading to more protective muscle coordination. Following this idea, our results suggest that the grip strategy G4 had lower TMC joint pressure. This decrease could be explained by the fact that this grip strategy (Table 1) led to a shift in the pressure distribution toward the central part of the trapezium, potentially allowing a more protective contact pattern. The pressure location shifting toward the central part may decrease the level of pressure due to more congruence between the surfaces in this zone. An illustration of this shift is provided in supplementary material (Figure 6–Supplementary Materials). This pressure decrease by performing a specific grip strategy could also explain the clinical improvement in managing OA pain with splinting techniques (Swigart et al. 1999). Joint posture modification induced by splinting can change the contact pattern and thus reduce pain in the joint. The insignificant effect of joint passive stiffness on the contact pressure of the TMC joint variation suggests that laxity might not be a risk factor for OA and corroborates a previous study (Halilaj et al. 2015).

Some limitations should be considered in this study. The dataset used to perform the sensitivity analysis was not the same between the three different factors and may contain some combinations of factors that are not possible to find in the real population. As discussed above, this could explain why some simulations did not converge. The use of an indirect estimation approach using FE-based modelling could be another limitation. Even if this approach is the only non-invasive alternative to investigate the numerous combinations of different factors on the joint contact pressure, such a model cannot be fully validated. A quantitative validation of the FE model by using pressor sensor measurements on cadaveric specimens (Athlani et al. 2022; Hwang et al. 2022) could be done but would still represent an estimation of the real pressure under natural *in vivo* movement. It should also be noted that only the pinch grip task was investigated in this study, whereas many other grasping tasks are used in everyday life and can lead to different TMC joint contact patterns (Schneider et al. 2017). Nevertheless, the pinch grip task has been largely associated with risks of developing hand OA (Jensen et al. 1999). Replicating the sensitivity analysis proposed here with another kind of grasping tasks like jar twist or power grip could be interesting to investigate whether the results observed during pinch grip are generalizable. Finally, cartilage modelling in the FE model was created by extruding the surface of the subchondral bones with a uniform thickness and material properties were considered homogeneous for the cartilage. Combining MRI with CT-scan to determine patient-specific material properties of cartilage could be another interesting future work to implement (Bayer et al. 2023). This approach could be interesting to investigate the contact area modification due to the non-linear behavior of the cartilage.

Despite these limitations, the sensitivity analysis performed in this study provided new insights into the different effects of three main parameters of the TMC joint. The results highlight the necessity to consider each patient-specific parameter (at least bone morphology and grip strategy considering their significant effects) to estimate the joint pressure correctly. Given the results observed, future studies need to develop patient-specific biomechanical models with longitudinal cohorts to simulate the pathological consequences of high mechanical loadings. This is the next step to understand OA development and potentially simulate surgical treatment by using computer simulations.

Authors contributions

All authors have made significant contribution to study design. Thomas Valerio, Laurent Vigouroux, Benjamin Goislard de Monsabert and Jean-Louis Milan contributed data analysis and interpretation. Development of the finite element simulations, drafting of the paper were performed by Thomas Valerio. All authors contributed critical revision of the paper and approved the final version of the manuscript to be published.

Disclosure statement

No potential conflict of interest was reported by the author(s).

Funding

The author(s) reported there is no funding associated with the work featured in this article.

ORCID

Thomas Valerio http://orcid.org/0000-0002-2758-9906

References

Ateshian GA, Rosenwasser MP, Mow VC. 1992. Curvature characteristics and congruence of the thumb carpometacarpal joint: differences between female and male joints. J Biomech. 25(6):591–607. doi: 10.1016/0021-9290(92)90102-7.

Athlani L, Auberson L, Motte D, Moissenet F, Beaulieu J-Y. 2021. Comparison of two radiographic landmarks for centering the trapezial component in total trapeziometacarpal arthroplasty. Hand Surg Rehabil. 40(5):609–613. doi: 10.1016/j.hansur.2021.05.002.

Athlani L, Bergere M, Motte D, Prandi B, Beaulieu J-Y, Moissenet F. 2022. Trapeziometacarpal joint loading during key pinch grip: a cadaver study. Hand Surg Rehabil. 41(2):204–209. doi: 10.1016/j.hansur.2021.11.009.

Barry AJ, Murray WM, Kamper DG. 2018. Development of a dynamic index finger and thumb model to study impairment. J Biomech. 77:206–210. doi: 10.1016/j.jbiomech.2018.06.017.

Bayer T, Brockhoff M-J, Nagel AM, Adler W, Lutter C, Janka R, Heiss R, Uder M, Roemer FW. 2023. Evaluation of finger cartilage composition in recreational climbers with 7 Tesla T2 mapping magnetic resonance imaging. Front Sports Act Living. 5:1248581. doi: 10.3389/fspor. 2023.1248581.

Besl PJ, McKay ND. 1992. A method for registration of 3-D shapes. IEEE Trans Pattern Anal Mach Intell. 14(2):239– 256. doi: 10.1109/34.121791.

Cerveri P, De Momi E, Marchente M, Baud-Bovy G, Scifo P, Barros RML, Ferrigno G. 2010. Method for the estimation of a double hinge kinematic model for the trapeziometacarpal joint using MR imaging. Comput Methods Biomech Biomed Eng. 13(3):387–396. doi: 10.1080/ 10255840903260818.

Cvijetic S, Kurtagic N, Ozegovic DD. 2004. Osteoarthritis of the hands in the rural population: a follow-up study. Eur J Epidemiol. 19(7):687–691. doi: 10.1023/b:ejep.0000036794.40723.8e.

Dong M, Kerkhof F, Deleu G, Vereecke E, Ladd A. 2023. Using a finite element model of the thumb to study Trapeziometacarpal joint contact during lateral pinch. Clin Biomech (Bristol, Avon). 101:105852. doi: 10.1016/j.clinbiomech.2022.105852.

Dourthe B, Nickmanesh R, Wilson DR, D'Agostino P, Patwa AN, Grinstaff MW, Snyder BD, Vereecke E., 2019. Assessment of healthy trapeziometacarpal cartilage properties using indentation testing and contrast-enhanced computed tomography. Clin Biomech (Bristol, Avon). 61:181– 189. doi: 10.1016/j.clinbiomech.2018.12.015.

Droz-Bartholet F, Verhoeven F, Prati C, Wendling D. 2016. Prevention of hand osteoarthritis by hemiparesis. Arthritis Rheumatol. 68(3):647–647. doi: 10.1002/art.39512.

Espino DM, Meakin JR, Hukins DWL, Reid JE. 2003. Stochastic finite element analysis of biological systems: comparison of a simple intervertebral disc model with experimental results. Comput Methods Biomech Biomed Eng. 6(4):243–248. doi: 10.1080/1025584031000160671.

Faudot B, Milan J-L, Goislard de Monsabert B, Le Corroller T, Vigouroux L. 2020. Estimation of joint contact pressure in the index finger using a hybrid finite element musculoskeletal approach. Comput Methods Biomech Biomed Eng. 23(15):1225–1235. doi: 10.1080/10255842.2020.1793965.

Felson DT. 2013. Osteoarthritis as a disease of mechanics. Osteoarthritis Cartilage. 21(1):10–15. doi: 10.1016/j.joca.2012.09.012.

Goislard de Monsabert B, Vigouroux L, Bendahan D, Berton E. 2014. Quantification of finger joint loadings using musculoskeletal modelling clarifies mechanical risk factors of hand osteoarthritis. Med Eng Phys. 36(2):177– 184. doi: 10.1016/j.medengphy.2013.10.007.

Halilaj E, Moore DC, Laidlaw DH, Got CJ, Weiss A-PC, Ladd AL, Crisco JJ. 2014. The morphology of the thumb carpometacarpal joint does not differ between men and women, but changes with aging and early osteoarthritis. J Biomech. 47(11):2709–2714. doi: 10.1016/j.jbiomech.2014.05.005.

Halilaj E, Moore DC, Patel TK, Ladd AL, Weiss AC, Crisco JJ. 2015. Early osteoarthritis of the trapeziometacarpal joint is not associated with joint instability during typical isometric loading. J Orthop Res. 33(11):1639–1645. doi: 10.1002/jor.22936.

Hwang JS, Li Q, Kim J. 2022. A quantitative measurement of trapeziometacarpal joint pressure using a cadaveric model of lateral pinch. J Orthop Res. 40(7):1523–1528. doi: 10.1002/jor.25188.

Jensen V, Bøggild H, Johansen JP. 1999. Occupational use of precision grip and forceful gripping, and arthrosis of finger joints: a literature review. Occup Med (Lond). 49(6):383–388. doi: 10.1093/occmed/49.6.383. Jonsson H, Eliasson GJ, Jonsson A, Eiríksdottir G, Sigurdsson S, Aspelund T, Harris TB, Gudnason V. 2009. High hand joint mobility is associated with radiological CMC1 osteoarthritis: the AGES-Reykjavik study. Osteoarthritis Cartilage. 17(5):592–595., doi: 10.1016/j.joca.2008.10.002.

Kempson GE. 1972. Mechanical properties of articular cartilage. J Physiol. 223(1):23P.

Koff MF, Ugwonali OF, Strauch RJ, Rosenwasser MP, Ateshian GA, Mow VC. 2003. Sequential wear patterns of the articular cartilage of the thumb carpometacarpal joint in osteoarthritis. J Hand Surg Am. 28(4):597–604. doi: 10.1016/S0363-5023(03)00145-X.

Kurosawa A, Higuchi M, Tachiya H, Tada K, Murai A, Tamai A, Kawashima H. 2024. Finite element analysis to clarify stress on articular surface of thumb carpometacarpal joint in static loading conditions by using CT images. JBSE. 19(2):23–00296–23-00296. doi: 10.1299/jbse.23-00296.

Ladd AL, Crisco JJ, Hagert E, Rose J, Weiss A-PC. 2014. The 2014 ABJS Nicolas Andry Award: the puzzle of the thumb: mobility, stability, and demands in opposition. Clin Orthop Relat Res. 472(12):3605–3622. doi: 10.1007/ s11999-014-3901-6.

Maas SA, Ellis BJ, Ateshian GA, Weiss JA. 2012. FEBio: finite elements for biomechanics. J Biomech Eng. 134(1): 011005. doi: 10.1115/1.4005694.

Mangado N, Piella G, Noailly J, Pons-Prats J, Ballester MAG. 2016. Analysis of uncertainty and variability in finite

element computational models for biomedical engineering: characterization and propagation. Front Bioeng Biotechnol. 4:85. doi: 10.3389/fbioe.2016.00085.

Moriatis Wolf J, Turkiewicz A, Atroshi I, Englund M. 2014. Prevalence of doctor-diagnosed thumb carpometacarpal joint osteoarthritis: an analysis of Swedish health care. Arthritis Care Res (Hoboken). 66(6):961–965. doi: 10.1002/acr.22250.

Rusli WMR, Kedgley AE. 2020. Statistical shape modelling of the first carpometacarpal joint reveals high variation in morphology. Biomech Model Mechanobiol. 19(4): 1203–1210. doi: 10.1007/s10237-019-01257-8.

Schneider MTY, Zhang J, Crisco JJ, Weiss A-PC, Ladd AL, Mithraratne K, Nielsen P, Besier T. 2017. Trapeziometacarpal joint contact varies between men and women during three isometric functional tasks. Med Eng Phys. 50: 43–49. doi: 10.1016/j.medengphy.2017.09.002.

Sciacca D, D'Agostino P, Vanneste M, Kerkhof F, Vereecke EE., 2022. In vivo quantification of the 3D kinematics and coupling of the thumb base joints. Med Eng Phys. 106:103837. doi: 10.1016/j.medengphy.2022.103837.

Shih JG, Mainprize JG, Binhammer PA. 2018. Comparison of computed tomography articular surface geometry of male versus female thumb carpometacarpal joints. Hand (N Y). 13(1):33–39. doi: 10.1177/1558944716688528.

Sim B, Lee J, Lee CG, Song H. 2022. Radiographic hand osteoarthritis in women farmers: characteristics and risk factors. Ann Occup Environ Med. 34(1):e10. doi: 10.35371/aoem.2022.34.e10.

Swigart CR, Eaton RG, Glickel SZ, Johnson C. 1999. Splinting in the treatment of arthritis of the first carpometacarpal joint. J Hand Surg Am. 24(1):86–91. doi: 10.1053/jhsu.1999.jhsu24a0086.

Valerio T, Milan J-L, Goislard De Monsabert B, Vigouroux L. 2024. The effect of trapeziometacarpal joint passive stiffness on mechanical loadings of cartilages. J Biomech. 166:112042. doi: 10.1016/j.jbiomech.2024.112042.

Valerio T, Vigouroux L, Goislard de Monsabert B, De Villeneuve Bargemon J-B, Milan J-L. 2023. Relationship between trapeziometacarpal joint morphological parameters and joint contact pressure: a possible factor of osteoarthritis development. J Biomech. 152:111573. doi: 10.1016/j.jbiomech.2023.111573.

Van Arkel RJ, Modenese L, Phillips ATM, Jeffers JRT. 2013. Hip abduction can prevent posterior edge loading of hip replacements. J Orthop Res. 31(8):1172–1179. doi: 10.1002/jor.22364.

van Leeuwen T, van Lenthe GH, Vereecke EE, Schneider MT. 2021. Stress distribution in the bonobo (*Pan paniscus*) trapeziometacarpal joint during grasping. PeerJ. 9: e12068. doi: 10.7717/peerj.12068.

Xu L, Strauch RJ, Ateshian GA, Pawluk RJ, Mow VC, Rosenwasser MP. 1998. Topography of the osteoarthritic thumb carpometacarpal joint and its variations with regard to gender, age, site, and osteoarthritic stage. J Hand Surg Am. 23(3):454–464. doi: 10.1016/S0363-5023(05)80463-0.

Yang K, Teo E-C, Fuss FK. 2007. Application of Taguchi method in optimization of cervical ring cage. J Biomech. 40(14):3251–3256. doi: 10.1016/j.jbiomech.2006.12.016.

Zimmerman BK, Ateshian GA. 2018. A surface-to-surface finite element algorithm for large deformation frictional contact in febio. J Biomech Eng. 140(8):0810131– 08101315. doi: 10.1115/1.4040497.